Version 1.6 as of February 8, 2007
Primary author: A. Haas

Comment to d0-run2eb-020@fnal.gov
by XXX, 2007

Search for Stopped Gluinos from $p\bar{p}$ Collisions at $\sqrt{s}$ =1.96 TeV

V.M. Abazov,[35] B. Abbott,[75] M. Abolins,[65] B.S. Acharya,[28] M. Adams,[51] T. Adams,[49] E. Aguilo,[5] S.H. Ahn,[30] M. Ahsan,[59] G.D. Alexeev,[35] G. Alkhazov,[39] A. Alton,[64,*] G. Alverson,[63] G.A. Alves,[2] M. Anastasoaie,[34] L.S. Ancu,[34] T. Andeen,[53] S. Anderson,[45] B. Andrieu,[16] M.S. Anzelc,[53] Y. Arnoud,[13] M. Arov,[52] A. Askew,[49] B. Åsman,[40] A.C.S. Assis Jesus,[3] O. Atramentov,[49] C. Autermann,[20] C. Avila,[7] C. Ay,[23] F. Badaud,[12] A. Baden,[61] L. Bagby,[52] B. Baldin,[50] D.V. Bandurin,[59] P. Banerjee,[28] S. Banerjee,[28] E. Barberis,[63] A.-F. Barfuss,[14] P. Bargassa,[80] P. Baringer,[58] J. Barreto,[2] J.F. Bartlett,[50] U. Bassler,[16] D. Bauer,[43] S. Beale,[5] A. Bean,[58] M. Begalli,[3] M. Begel,[71] C. Belanger-Champagne,[40] L. Bellantoni,[50] A. Bellavance,[67] J.A. Benitez,[65] S.B. Beri,[26] G. Bernardi,[16] R. Bernhard,[22] L. Berntzon,[14] I. Bertram,[42] M. Besançon,[17] R. Beuselinck,[43] V.A. Bezzubov,[38] P.C. Bhat,[50] V. Bhatnagar,[26] M. Binder,[24] C. Biscarat,[19] G. Blazey,[52] F. Blekman,[43] S. Blessing,[49] D. Bloch,[18] K. Bloom,[67] A. Boehnlein,[50] D. Boline,[62] T.A. Bolton,[59] G. Borissov,[42] K. Bos,[33] T. Bose,[77] A. Brandt,[78] R. Brock,[65] G. Brooijmans,[70] A. Bross,[50] D. Brown,[78] N.J. Buchanan,[49] D. Buchholz,[53] M. Buehler,[81] V. Buescher,[21] S. Burdin,[50] S. Burke,[45] T.H. Burnett,[82] E. Busato,[16] C.P. Buszello,[43] J.M. Butler,[62] P. Calfayan,[24] S. Calvet,[14] J. Cammin,[71] S. Caron,[33] W. Carvalho,[3] B.C.K. Casey,[77] N.M. Cason,[55] H. Castilla-Valdez,[32] S. Chakrabarti,[17] D. Chakraborty,[52] K. Chan,[5] K.M. Chan,[71] A. Chandra,[48] F. Charles,[18] E. Cheu,[45] F. Chevallier,[13] D.K. Cho,[62] S. Choi,[31] B. Choudhary,[27] L. Christofek,[77] T. Christoudias,[43] S. Cihangir,[50] D. Claes,[67] B. Clément,[18] C. Clément,[40] Y. Coadou,[5] M. Cooke,[80] W.E. Cooper,[50] M. Corcoran,[80] F. Couderc,[17] M.-C. Cousinou,[14] S. Crépé-Renaudin,[13] D. Cutts,[77] M. Ćwiok,[29] H. da Motta,[2] A. Das,[62] G. Davies,[43] K. De,[78] P. de Jong,[33] S.J. de Jong,[34] E. De La Cruz-Burelo,[64] C. De Oliveira Martins,[3] J.D. Degenhardt,[64] F. Déliot,[17] M. Demarteau,[50] R. Demina,[71] D. Denisov,[50] S.P. Denisov,[38] S. Desai,[50] H.T. Diehl,[50] M. Diesburg,[50] A. Dominguez,[67] H. Dong,[72] L.V. Dudko,[37] L. Duflot,[15] S.R. Dugad,[28] D. Duggan,[49] A. Duperrin,[14] J. Dyer,[65] A. Dyshkant,[52] M. Eads,[67] D. Edmunds,[65] J. Ellison,[48] V.D. Elvira,[50] Y. Enari,[77] S. Eno,[61] P. Ermolov,[37] H. Evans,[54] A. Evdokimov,[36] V.N. Evdokimov,[38] A.V. Ferapontov,[59] T. Ferbel,[71] F. Fiedler,[24] F. Filthaut,[34] W. Fisher,[50] H.E. Fisk,[50] M. Ford,[44] M. Fortner,[52] H. Fox,[22] S. Fu,[50] S. Fuess,[50] T. Gadfort,[82] C.F. Galea,[34] E. Gallas,[50] E. Galyaev,[55] C. Garcia,[71] A. Garcia-Bellido,[82] V. Gavrilov,[36] P. Gay,[12] W. Geist,[18] D. Gelé,[18] C.E. Gerber,[51] Y. Gershtein,[49] D. Gillberg,[5] G. Ginther,[71] N. Gollub,[40] B. Gómez,[7] A. Goussiou,[55] P.D. Grannis,[72] H. Greenlee,[50] Z.D. Greenwood,[60] E.M. Gregores,[4] G. Grenier,[19] Ph. Gris,[12] J.-F. Grivaz,[15] A. Grohsjean,[24] S. Grünendahl,[50] M.W. Grünewald,[29] F. Guo,[72] J. Guo,[72] G. Gutierrez,[50] P. Gutierrez,[75] A. Haas,[70] N.J. Hadley,[61] P. Haefner,[24] S. Hagopian,[49] J. Haley,[68] I. Hall,[75] R.E. Hall,[47] L. Han,[6] K. Hanagaki,[50] P. Hansson,[40] K. Harder,[44] A. Harel,[71] R. Harrington,[63] J.M. Hauptman,[57] R. Hauser,[65] J. Hays,[43] T. Hebbeker,[20] D. Hedin,[52] J.G. Hegeman,[33] J.M. Heinmiller,[51] A.P. Heinson,[48] U. Heintz,[62] C. Hensel,[58] K. Herner,[72] G. Hesketh,[63] M.D. Hildreth,[55] R. Hirosky,[81] J.D. Hobbs,[72] B. Hoeneisen,[11] H. Hoeth,[25] M. Hohlfeld,[15] S.J. Hong,[30] R. Hooper,[77] P. Houben,[33] Y. Hu,[72] Z. Hubacek,[9] V. Hynek,[8] I. Iashvili,[69] R. Illingworth,[50] A.S. Ito,[50] S. Jabeen,[62] M. Jaffré,[15] S. Jain,[75] K. Jakobs,[22] C. Jarvis,[61] R. Jesik,[43] K. Johns,[45] C. Johnson,[70] M. Johnson,[50] A. Jonckheere,[50] P. Jonsson,[43] A. Juste,[50] D. Käfer,[20] S. Kahn,[73] E. Kajfasz,[14] A.M. Kalinin,[35] J.M. Kalk,[60] J.R. Kalk,[65] S. Kappler,[20] D. Karmanov,[37] J. Kasper,[62] P. Kasper,[50] I. Katsanos,[70] D. Kau,[49] R. Kaur,[26] V. Kaushik,[78] R. Kehoe,[79] S. Kermiche,[14] N. Khalatyan,[38] A. Khanov,[76] A. Kharchilava,[69] Y.M. Kharzheev,[35] D. Khatidze,[70] H. Kim,[31] T.J. Kim,[30] M.H. Kirby,[34] B. Klima,[50] J.M. Kohli,[26] J.-P. Konrath,[22] M. Kopal,[75] V.M. Korablev,[38] J. Kotcher,[73] B. Kothari,[70] A. Koubarovsky,[37] A.V. Kozelov,[38] D. Krop,[54] A. Kryemadhi,[81] T. Kuhl,[23] A. Kumar,[69] S. Kunori,[61] A. Kupco,[10] T. Kurča,[19] J. Kvita,[8] D. Lam,[55] S. Lammers,[70] G. Landsberg,[77] J. Lazoflores,[49] P. Lebrun,[19] W.M. Lee,[50] A. Leflat,[37] F. Lehner,[41] V. Lesne,[12] J. Leveque,[45] P. Lewis,[43] J. Li,[78] L. Li,[48] Q.Z. Li,[50] S.M. Lietti,[4] J.G.R. Lima,[52] D. Lincoln,[50] J. Linnemann,[65] V.V. Lipaev,[38] R. Lipton,[50] Z. Liu,[5] L. Lobo,[43] A. Lobodenko,[39] M. Lokajicek,[10] A. Lounis,[18] P. Love,[42] H.J. Lubatti,[82] M. Lynker,[55] A.L. Lyon,[50] A.K.A. Maciel,[2] R.J. Madaras,[46] P. Mättig,[25] C. Magass,[20] A. Magerkurth,[64] N. Makovec,[15] P.K. Mal,[55] H.B. Malbouisson,[3] S. Malik,[67] V.L. Malyshev,[35] H.S. Mao,[50] Y. Maravin,[59] B. Martin,[13] R. McCarthy,[72] A. Melnitchouk,[66] A. Mendes,[14] L. Mendoza,[7] P.G. Mercadante,[4] M. Merkin,[37] K.W. Merritt,[50] A. Meyer,[20] J. Meyer,[21] M. Michaut,[17] H. Miettinen,[80] T. Millet,[19] J. Mitrevski,[70] J. Molina,[3] R.K. Mommsen,[44] N.K. Mondal,[28] J. Monk,[44] R.W. Moore,[5] T. Moulik,[58] G.S. Muanza,[19] M. Mulders,[50] M. Mulhearn,[70] O. Mundal,[21] L. Mundim,[3] E. Nagy,[14]

M. Naimuddin,[50] M. Narain,[77] N.A. Naumann,[34] H.A. Neal,[64] J.P. Negret,[7] P. Neustroev,[39] H. Nilsen,[22] C. Noeding,[22] A. Nomerotski,[50] S.F. Novaes,[4] T. Nunnemann,[24] V. O'Dell,[50] D.C. O'Neil,[5] G. Obrant,[39] C. Ochando,[15] V. Oguri,[3] N. Oliveira,[3] D. Onoprienko,[59] N. Oshima,[50] J. Osta,[55] R. Otec,[9] G.J. Otero y Garzón,[51] M. Owen,[44] P. Padley,[80] M. Pangilinan,[77] N. Parashar,[56] S.-J. Park,[71] S.K. Park,[30] J. Parsons,[70] R. Partridge,[77] N. Parua,[72] A. Patwa,[73] G. Pawloski,[80] P.M. Perea,[48] K. Peters,[44] Y. Peters,[25] P. Pétroff,[15] M. Petteni,[43] R. Piegaia,[1] J. Piper,[65] M.-A. Pleier,[21] P.L.M. Podesta-Lerma,[32,§] V.M. Podstavkov,[50] Y. Pogorelov,[55] M.-E. Pol,[2] A. Pompoš,[75] B.G. Pope,[65] A.V. Popov,[38] C. Potter,[5] W.L. Prado da Silva,[3] H.B. Prosper,[49] S. Protopopescu,[73] J. Qian,[64] A. Quadt,[21] B. Quinn,[66] M.S. Rangel,[2] K.J. Rani,[28] K. Ranjan,[27] P.N. Ratoff,[42] P. Renkel,[79] S. Reucroft,[63] M. Rijssenbeek,[72] I. Ripp-Baudot,[18] F. Rizatdinova,[76] S. Robinson,[43] R.F. Rodrigues,[3] C. Royon,[17] P. Rubinov,[50] R. Ruchti,[55] G. Sajot,[13] A. Sánchez-Hernández,[32] M.P. Sanders,[16] A. Santoro,[3] G. Savage,[50] L. Sawyer,[60] T. Scanlon,[43] D. Schaile,[24] R.D. Schamberger,[72] Y. Scheglov,[39] H. Schellman,[53] P. Schieferdecker,[24] C. Schmitt,[25] C. Schwanenberger,[44] A. Schwartzman,[68] R. Schwienhorst,[65] J. Sekaric,[49] S. Sengupta,[49] H. Severini,[75] E. Shabalina,[51] M. Shamim,[59] V. Shary,[17] A.A. Shchukin,[38] R.K. Shivpuri,[27] D. Shpakov,[50] V. Siccardi,[18] R.A. Sidwell,[59] V. Simak,[9] V. Sirotenko,[50] P. Skubic,[75] P. Slattery,[71] D. Smirnov,[55] R.P. Smith,[50] G.R. Snow,[67] J. Snow,[74] S. Snyder,[73] S. Söldner-Rembold,[44] L. Sonnenschein,[16] A. Sopczak,[42] M. Sosebee,[78] K. Soustruznik,[8] M. Souza,[2] B. Spurlock,[78] J. Stark,[13] J. Steele,[60] V. Stolin,[36] D.A. Stoyanova,[38] J. Strandberg,[64] S. Strandberg,[40] M.A. Strang,[69] M. Strauss,[75] R. Ströhmer,[24] D. Strom,[53] M. Strovink,[46] L. Stutte,[50] S. Sumowidagdo,[49] P. Svoisky,[55] A. Sznajder,[3] M. Talby,[14] P. Tamburello,[45] A. Tanasijczuk,[1] W. Taylor,[5] P. Telford,[44] J. Temple,[45] B. Tiller,[24] F. Tissandier,[12] M. Titov,[22] V.V. Tokmenin,[35] M. Tomoto,[50] T. Toole,[61] I. Torchiani,[22] T. Trefzger,[23] S. Trincaz-Duvoid,[16] D. Tsybychev,[72] B. Tuchming,[17] C. Tully,[68] P.M. Tuts,[70] R. Unalan,[65] L. Uvarov,[39] S. Uvarov,[39] S. Uzunyan,[52] B. Vachon,[5] P.J. van den Berg,[33] B. van Eijk,[35] R. Van Kooten,[54] W.M. van Leeuwen,[33] N. Varelas,[51] E.W. Varnes,[45] A. Vartapetian,[78] I.A. Vasilyev,[38] M. Vaupel,[25] P. Verdier,[19] L.S. Vertogradov,[35] M. Verzocchi,[50] F. Villeneuve-Seguier,[43] P. Vint,[43] J.-R. Vlimant,[16] E. Von Toerne,[59] M. Voutilainen,[67,‡] M. Vreeswijk,[33] H.D. Wahl,[49] L. Wang,[61] M.H.L.S Wang,[50] J. Warchol,[55] G. Watts,[82] M. Wayne,[55] G. Weber,[23] M. Weber,[50] H. Weerts,[65] A. Wenger,[22,#] N. Wermes,[21] M. Wetstein,[61] A. White,[78] D. Wicke,[25] G.W. Wilson,[58] S.J. Wimpenny,[48] M. Wobisch,[50] D.R. Wood,[63] T.R. Wyatt,[44] Y. Xie,[77] S. Yacoob,[53] R. Yamada,[50] M. Yan,[61] T. Yasuda,[50] Y.A. Yatsunenko,[35] K. Yip,[73] H.D. Yoo,[77] S.W. Youn,[53] C. Yu,[13] J. Yu,[78] A. Yurkewicz,[72] A. Zatserklyaniy,[52] C. Zeitnitz,[25] D. Zhang,[50] T. Zhao,[82] B. Zhou,[64] J. Zhu,[72] M. Zielinski,[71] D. Zieminska,[54] A. Zieminski,[54] V. Zutshi,[52] and E.G. Zverev[37]

(DØ Collaboration)

[1] *Universidad de Buenos Aires, Buenos Aires, Argentina*
[2] *LAFEX, Centro Brasileiro de Pesquisas Físicas, Rio de Janeiro, Brazil*
[3] *Universidade do Estado do Rio de Janeiro, Rio de Janeiro, Brazil*
[4] *Instituto de Física Teórica, Universidade Estadual Paulista, São Paulo, Brazil*
[5] *University of Alberta, Edmonton, Alberta, Canada, Simon Fraser University, Burnaby, British Columbia, Canada, York University, Toronto, Ontario, Canada, and McGill University, Montreal, Quebec, Canada*
[6] *University of Science and Technology of China, Hefei, People's Republic of China*
[7] *Universidad de los Andes, Bogotá, Colombia*
[8] *Center for Particle Physics, Charles University, Prague, Czech Republic*
[9] *Czech Technical University, Prague, Czech Republic*
[10] *Center for Particle Physics, Institute of Physics, Academy of Sciences of the Czech Republic, Prague, Czech Republic*
[11] *Universidad San Francisco de Quito, Quito, Ecuador*
[12] *Laboratoire de Physique Corpusculaire, IN2P3-CNRS, Université Blaise Pascal, Clermont-Ferrand, France*
[13] *Laboratoire de Physique Subatomique et de Cosmologie, IN2P3-CNRS, Universite de Grenoble 1, Grenoble, France*
[14] *CPPM, IN2P3-CNRS, Université de la Méditerranée, Marseille, France*
[15] *Laboratoire de l'Accélérateur Linéaire, IN2P3-CNRS et Université Paris-Sud, Orsay, France*
[16] *LPNHE, IN2P3-CNRS, Universités Paris VI and VII, Paris, France*
[17] *DAPNIA/Service de Physique des Particules, CEA, Saclay, France*
[18] *IPHC, IN2P3-CNRS, Université Louis Pasteur, Strasbourg, France, and Université de Haute Alsace, Mulhouse, France*
[19] *IPNL, Université Lyon 1, CNRS/IN2P3, Villeurbanne, France and Université de Lyon, Lyon, France*
[20] *III. Physikalisches Institut A, RWTH Aachen, Aachen, Germany*
[21] *Physikalisches Institut, Universität Bonn, Bonn, Germany*
[22] *Physikalisches Institut, Universität Freiburg, Freiburg, Germany*
[23] *Institut für Physik, Universität Mainz, Mainz, Germany*
[24] *Ludwig-Maximilians-Universität München, München, Germany*
[25] *Fachbereich Physik, University of Wuppertal, Wuppertal, Germany*
[26] *Panjab University, Chandigarh, India*

[27] *Delhi University, Delhi, India*
[28] *Tata Institute of Fundamental Research, Mumbai, India*
[29] *University College Dublin, Dublin, Ireland*
[30] *Korea Detector Laboratory, Korea University, Seoul, Korea*
[31] *SungKyunKwan University, Suwon, Korea*
[32] *CINVESTAV, Mexico City, Mexico*
[33] *FOM-Institute NIKHEF and University of Amsterdam/NIKHEF, Amsterdam, The Netherlands*
[34] *Radboud University Nijmegen/NIKHEF, Nijmegen, The Netherlands*
[35] *Joint Institute for Nuclear Research, Dubna, Russia*
[36] *Institute for Theoretical and Experimental Physics, Moscow, Russia*
[37] *Moscow State University, Moscow, Russia*
[38] *Institute for High Energy Physics, Protvino, Russia*
[39] *Petersburg Nuclear Physics Institute, St. Petersburg, Russia*
[40] *Lund University, Lund, Sweden, Royal Institute of Technology and Stockholm University, Stockholm, Sweden, and Uppsala University, Uppsala, Sweden*
[41] *Physik Institut der Universität Zürich, Zürich, Switzerland*
[42] *Lancaster University, Lancaster, United Kingdom*
[43] *Imperial College, London, United Kingdom*
[44] *University of Manchester, Manchester, United Kingdom*
[45] *University of Arizona, Tucson, Arizona 85721, USA*
[46] *Lawrence Berkeley National Laboratory and University of California, Berkeley, California 94720, USA*
[47] *California State University, Fresno, California 93740, USA*
[48] *University of California, Riverside, California 92521, USA*
[49] *Florida State University, Tallahassee, Florida 32306, USA*
[50] *Fermi National Accelerator Laboratory, Batavia, Illinois 60510, USA*
[51] *University of Illinois at Chicago, Chicago, Illinois 60607, USA*
[52] *Northern Illinois University, DeKalb, Illinois 60115, USA*
[53] *Northwestern University, Evanston, Illinois 60208, USA*
[54] *Indiana University, Bloomington, Indiana 47405, USA*
[55] *University of Notre Dame, Notre Dame, Indiana 46556, USA*
[56] *Purdue University Calumet, Hammond, Indiana 46323, USA*
[57] *Iowa State University, Ames, Iowa 50011, USA*
[58] *University of Kansas, Lawrence, Kansas 66045, USA*
[59] *Kansas State University, Manhattan, Kansas 66506, USA*
[60] *Louisiana Tech University, Ruston, Louisiana 71272, USA*
[61] *University of Maryland, College Park, Maryland 20742, USA*
[62] *Boston University, Boston, Massachusetts 02215, USA*
[63] *Northeastern University, Boston, Massachusetts 02115, USA*
[64] *University of Michigan, Ann Arbor, Michigan 48109, USA*
[65] *Michigan State University, East Lansing, Michigan 48824, USA*
[66] *University of Mississippi, University, Mississippi 38677, USA*
[67] *University of Nebraska, Lincoln, Nebraska 68588, USA*
[68] *Princeton University, Princeton, New Jersey 08544, USA*
[69] *State University of New York, Buffalo, New York 14260, USA*
[70] *Columbia University, New York, New York 10027, USA*
[71] *University of Rochester, Rochester, New York 14627, USA*
[72] *State University of New York, Stony Brook, New York 11794, USA*
[73] *Brookhaven National Laboratory, Upton, New York 11973, USA*
[74] *Langston University, Langston, Oklahoma 73050, USA*
[75] *University of Oklahoma, Norman, Oklahoma 73019, USA*
[76] *Oklahoma State University, Stillwater, Oklahoma 74078, USA*
[77] *Brown University, Providence, Rhode Island 02912, USA*
[78] *University of Texas, Arlington, Texas 76019, USA*
[79] *Southern Methodist University, Dallas, Texas 75275, USA*
[80] *Rice University, Houston, Texas 77005, USA*
[81] *University of Virginia, Charlottesville, Virginia 22901, USA*
[82] *University of Washington, Seattle, Washington 98195, USA*

(Dated: February 8, 2007)

A long-lived, colored, heavy particle is predicted in several models of beyond the Standard Model physics, the prime example being the gluino in Split-Supersymmetry. Gluinos carry color charge and are thus expected to hadronize into colorless bound states called R-hadrons. Some fraction of the R-hadrons can become charged and lose enough momentum through ionization to come to rest

in dense particle detectors. Approximately 410 pb^{-1} of $p\bar{p}$ collisions at $\sqrt{s}$ = 1960 GeV collected with the DØ detector during Run II of the Fermilab Tevatron is analyzed in search of such "stopped gluinos" (G) decaying into a gluon and a neutralino, reconstructed as a jet and missing energy. No excess is observed above the expected background from cosmic-muons, and limits are placed on the (gluino cross-section) × (probability to stop) × (BR(G→$g\chi_1^0$)) as a function of the gluino and neutralino masses, for gluino lifetimes from 30μs - 100 hours.

PACS numbers:

Split-Supersymmetry is a relatively new variant of Supersymmetry, in which the Supersymmetric scalars are heavy (possibly GUT-scale) compared to the (SUSY) fermions [1]. Due to the scalars' high masses, the gluino decays are suppressed, and it can be long-lived. The gluinos hadronize into "R-hadrons", colorless bound states of a gluino and other quarks or gluons. At the Tevatron, gluinos could be pair produced through strong interactions. If $M_{SUSY} > 10^6$ GeV, the R-hadrons live long enough (>10 ns) to reach the DØ calorimeters. As studied in [3], some charged R-hadrons can become such "stopped gluinos", by losing all of their momentum through ionization and coming to rest in the calorimeters.

This analysis searches for stopped gluinos decaying into a gluon and a neutralino. The gluino lifetime is assumed to be long enough such that the decay occurs during a bunch-crossing later than the one which produced it (at least 30 μs). The efficiency for recording the gluino decay is modeled as a function of the gluino lifetime, up to a lifetime of 100 hours. When the decay occurs during a bunch-crossing with very little other high-p_T activity, the signal signature is a largely empty event with a single high-energy deposit in the calorimeter, reconstructed as a jet and large missing transverse energy ($\not\!\!E_T$).

The radial location of the gluino when it decays depends on the way the gluinos lose energy via ionization and stop in the calorimeters. This calculation was performed [3] for a distribution of material similar to the DØ calorimeters and a gluino velocity distribution as expected from production at the Tevatron. The pseudo-rapidity (η) distribution is determined by the fact that gluinos would tend to be produced near threshold at the Tevatron, and that only slow gluinos would stop. Therefore the gluinos are expected to be distributed proportionally to $\sin\theta$, where θ is the angle from the z-axis or beamline. More than 75% of gluinos which stop are in $|\eta|$<1. The gluinos are at rest and randomly oriented in space when they decay; thus the gluon is emitted in a random direction. The energy of the gluon, which hadronizes and fragments into a jet, depends on the gluino and LSP masses:

$$E = (M_g^2 - M_{LSP}^2)/2M_g \qquad (1)$$

To simulate the jets that would be produced by stopped gluino decays, the PYTHIA [4] generator was used to produce Z+gluon events with the Z forced to decay to neutrinos. The location of the interaction point was placed inside the calorimeter, and events were further weighted such that the final decay position distributions are those expected for stopped gluinos as described above. Initial-state radiation was switched off in PYTHIA, and so were multiple parton interactions. The $|\eta|$ of the gluon was restricted to be less than 0.1 at the generator level. The spectator particles coming from the rest of the $p\bar{p}$ interaction, such as the underlying event, were removed at the generator stage by removing all particles with $|pz/E| > 0.95$. Finally, a random 3D rotation was applied to the remaining particles, to simulate the random decay axis of the gluino.

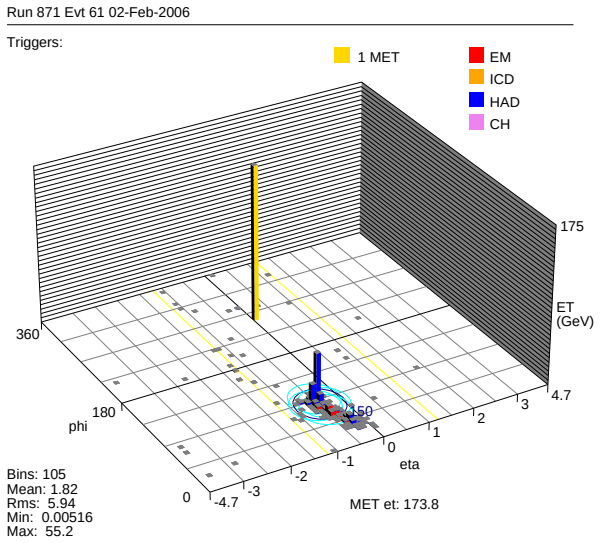

FIG. 1: A simulated stopped gluino decay event, for m_G=400 GeV. The height of each bar corresponds to the total E_T in that η x ϕ tower. The $\not\!\!E_T$ is shown as a yellow bar.

Four samples of stopped gluinos were made, containing about 1000 events each, using a GEANT-based detector simulation and reconstructed using the same algorithms as data. They correspond to gluino masses of 200, 300, 400, and 500 GeV, for an LSP mass of 90 GeV. Using Equation 1, we note that these samples thus correspond to generated parton energies of 80, 137, 190, and 242 GeV, respectively. An event display of a simulated stopped gluino decay is shown in Figure 1.

Data taken from November 2002 – August 2004, about 410 pb^{-1}, were reconstructed and analyzed. Since no $p\bar{p}$ beam-interaction is expected to be correlated with the

stopped gluino decay, the trigger for each event requires that neither the North nor South luminosity counters, placed on the front face of the end-cap calorimeters at high $|\eta|$, have fired. The trigger also requires at least two calorimeter towers with E_T>3 GeV and a reconstructed jet with E_T>15 GeV.

Jets were reconstructed with the Run II Improved Legacy Cone Algorithm (ILCA) [5] with cone size of ΔR=0.5. Simulated jets were corrected for relative differences between the data and MC jet energy scales. In addition, jet energies in the simulation were corrected (downwards) according to a model of the out-of-time calorimeter response, due to the fact that the calorimeter electronics sample the shaped ionization signal only once per bunch-crossing at the assumed peak of the signal. The average degradation of energy is 30%, although more than half the jets are not significantly degraded.

Muons were reconstructed, and no extra quality criteria or corrections were applied. The DØ muon detector system has three layers (A,B,C). The first (A) is inside the iron toroid magnet, while the second two (B,C) are outside it. Muons were separated according to whether they extended beyond the A-layer or not.

Loose cuts were used to select an initial data sample to study. We require exactly one jet in the event with E_T>8 GeV, and the jet must have E>90 GeV. This avoids noise jets and is also high enough such that the calorimeter part of the trigger is nearly 100% efficient.

The major source of background is cosmic muons, which are able to fake a gluino signal if they initiate a high-energy shower within the calorimeter. Hard bremsstrahlung emission is responsible for the majority of the showers. These showers tend to be very narrow, since they are electromagnetic in nature and thus have small interaction lengths compared to hadronic showers. Most of the energy is deposited in a few calorimeter cells, see Figure 2. However, sometimes a wide, hadronic-like, shower can be created either due to real deep-inelastic scattering, fluctuations of the shower, or detector effects.

Cosmic muons can usually be identified by the presence of a high-energy muon, either entering or exiting the detector, using the muon detectors. In particular, a coincidence of muon hits in the outer two (B,C) layers of the muon system are very strong evidence of a muon. The A-layer hits are often also caused by the signal, due to particles escaping the calorimeters, so these hits are difficult to use for background rejection. Sometimes the muon is not detected, due to detector inefficiencies or the limited detector acceptance, up to $|\eta|$<2. Muons can also be detected, in principle, through their ionizing interactions in the calorimeter, where they are minimum-ionizing particles (MIP's). However, these MIP trails are difficult to identify in this geometry where the direction of the muon path is unknown, and also there is a large shower nearby which overlaps with the energy deposited by the MIP.

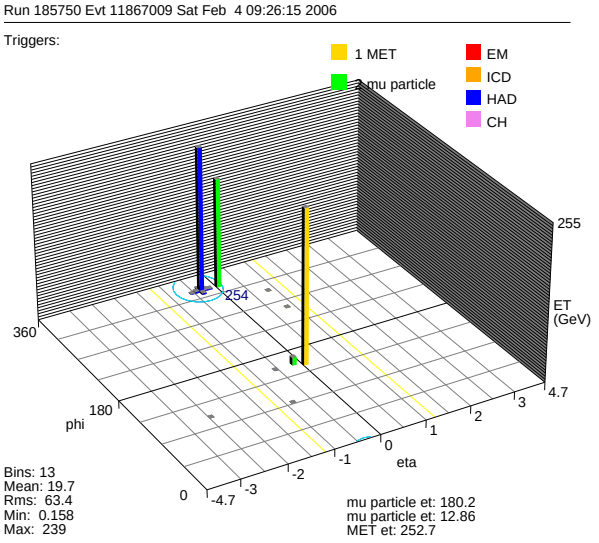

FIG. 2: A typical cosmic muon, hard Bremsstrahlung, shower. There are reconstructed muons (shown in green) and a very narrow energy deposit.

Another source of background events is beam-halo muons, or "beam-muons". These are muons, in-time with the $p\bar{p}$ bunches, and traveling nearly parallel to the beam. Often, a muon scintillator hit or two can be associated with the muon, and the muon can be seen to be in-time, with Δt<10 ns. Another feature of the beam-muons is that they are nearly all in the plane of the accelerator beam, i.e. with ϕ very near to integer multiples of π. Beam-muon showers are also typically very narrow in ϕ-width, even narrower than cosmic muon showers.

Since the trigger requires no firing of the luminosity counters, nearly all of the $p\bar{p}$ beam produced backgrounds are eliminated. An exception is double diffractive events with large momentum transfer. However, after requiring no primary vertex (PV) to be reconstructed and large $\not\!\!E_T$, these events are eliminated. Di-jet events in the same data sample were studied to understand the $\not\!\!E_T$ spectrum and PV reconstruction efficiency for beam-related backgrounds.

Other small sources of physics background considered were cosmic neutrons and neutrinos, both of which were determined to be negligible.

Finally, since the signal process is rare, one needs to consider occasional fake signal processes that could be caused by detector problems. However, these problems tend to be isolated to a specific set of runs, a specific detector region, or both, and such events are removed. We require the jet to be in $|\eta|$<0.9, since the forward regions of the calorimeter were observed to have more frequent (yet still rare) detector problems. Also, the gluino signal tends to be concentrated in the central regions. The rectangular region of the calorimeter ($-.55 < \eta < -.75$, $1.3 < \phi < 1.5$) was too noisy and therefore all events in that region were rejected.

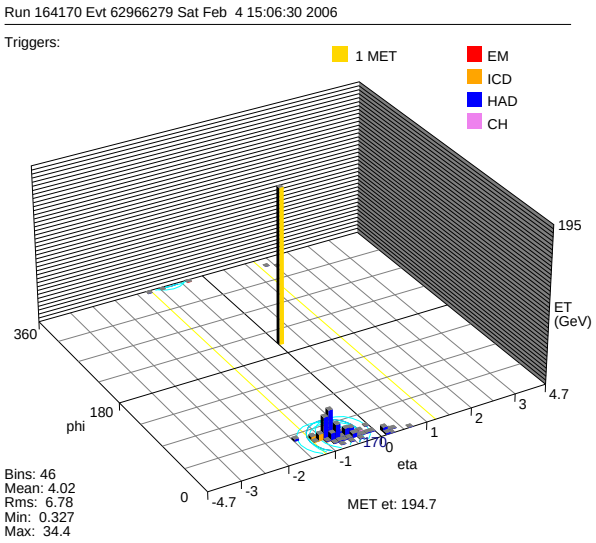

FIG. 3: A candidate signal event in data, containing a wide shower with no good muon.

The following criteria are used to select events containing "wide showers": jet η-width and ϕ-width >0.08 and jet n_{90} ≥10, where n_{90} is the smallest number of calorimeter cells in the jet that make up 90% of the jet energy. Criteria are also defined to select events containing "no muon". A candidate gluino shower would be both wide and contain no muon. Figure 3 shows a display of a candidate event.

To estimate the number of wide no-muon showers expected from background, we use the assumption that the probability not to reconstruct the cosmic muon is independent of whether the muon shower is narrow or wide. We first measure the probability to miss the muon (P_{nomu}) in the narrow-jet cosmic data sample, and determine P_{nomu}=0.11±0.01, independent of jet energy. This probability is applied to the wide-jet cosmic-muon data sample to predict the spectrum of wide-shower no-muon background events.

To first order, the detection efficiency for the decays of the stopped gluino signal events can be estimated from the MC simulation, but some effects are not modeled. There is a loss of efficiency at the trigger level from the no luminosity-counter requirement. If a min-bias event happens to occur during the bunch crossing when the gluino decays, a luminosity counter may fire. The fraction of the time this occurs has been measured using cosmic-muon shower events triggered on a jet-only trigger with higher threshold. The efficiency of the luminosity-counter trigger term, averaged over the data set, is 75%. The probability to have no min-bias interactions during a given crossing is proportional to $e^{-\lambda}$, where λ is the average number of interactions per crossing, which is proportional to the instantaneous luminosity. For this data set, $\lambda \simeq 0.3$ on average. A detailed model of the trigger

E. Range (GeV)	Data	Bgnd.	Eff.	Exp.(pb)	Obs.(pb)
92.5-104.6	30	37.07	0.017	2.61	1.81
112.4-156.6	39	40.26	0.049	0.94	0.89
141.3-213.0	34	30.91	0.068	0.56	0.71
168.7-270.6	32	25.74	0.072	0.48	0.75

TABLE I: The data, background, signal efficiency, and observed and expected limits (at 95% C.L.) for each jet energy range, for a small gluino lifetime: <3 hours.

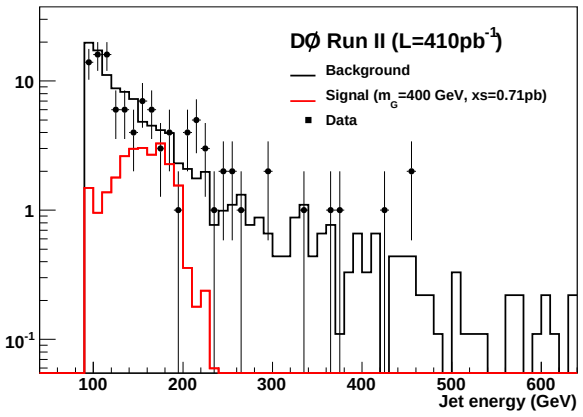

FIG. 4: A comparison of the wide-jet no-muon data (black points) to the expected background (black histogram), with log scale. Also shown is the signal simulated for m_G=400 GeV and m_{LSP}=90 GeV at the excluded limit of 0.7 pb (red histogram).

efficiency was made as a function of the gluino lifetime, for lifetimes up to 100 hours, using the typical Tevatron store luminosity profile as an input.

Another source of inefficiency is that the trigger is not live all the time, but only during the "live superbunches", which make up 68% of the total accelerator turn time, with minimal uncertainty.

The final efficiencies for detecting the stopped gluino decay are shown in Table I. The uncertainties from all sources which affect the signal acceptance are added in quadrature, totaling 20-25%. They include: the modeling of the out-of-time jet response (12%), the data/MC jet energy scale (9%), the η and radial distributions of stopped gluinos (7-9%), other geometrical or kinematic acceptances (5%), and trigger efficiency (5-15%).

Applying the measured P_{nomu} to the wide-jet cosmic-muon data sample, we estimate the energy spectrum of the expected wide-jet no-muon background, as shown in Figure 4 along with the observed wide-jet no-muon events in data. The estimated background predicts the data well, and there is no significant excess in data at any energy range.

Given an observed number of candidate events, an expected number of background events, and a signal ef-

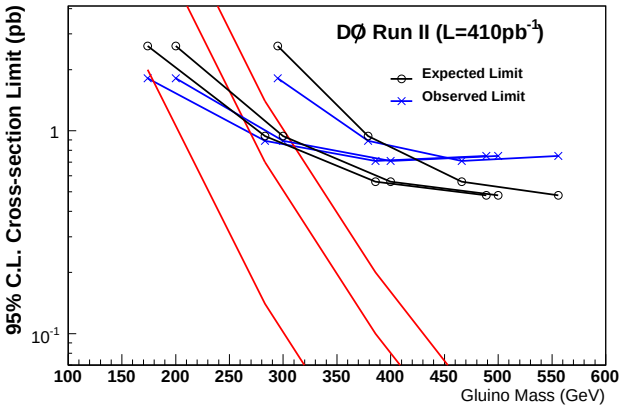

FIG. 5: The 95% C.L. upper limits expected (black, open circles) and observed (blue, crosses) on the cross-section of stopped gluinos decaying into a jet, assuming a 100% BR of G→g+LSP and a small gluino lifetime (<3 hours), for 3 choices of the simulated LSP mass: 50, 90 and 200 GeV, from left to right. Also shown is the theoretical cross-section (red, stars), from [3], for conversion cross-sections of 0.3, 3, and 30 mb.

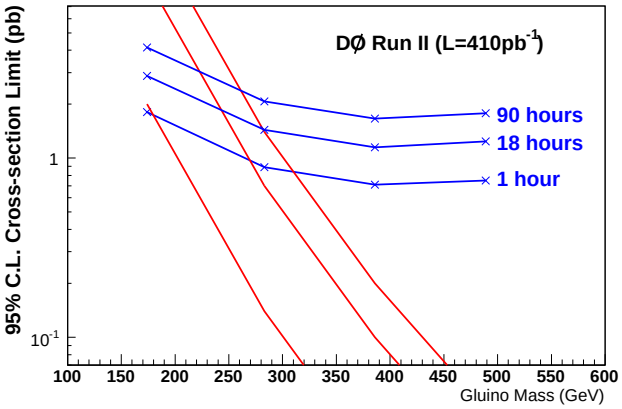

FIG. 6: The 95% C.L. upper limits observed on the cross-section of stopped gluinos decaying into a jet, for various assumptions of the gluino lifetime: 1, 18, and 90 hours, for an LSP mass of 50 GeV. Also shown is the theoretical cross-section (red, stars), from [3], for conversion cross-sections of 0.3, 3, and 30 mb.

ficiency in a certain jet energy bin, we can exclude at 95% C.L. a calculated rate of signal events giving jets of that energy, taking systematic uncertainties into account. This is a fairly model-independent result, limiting the rate of any out-of-time mono-jet signal of a given energy. From there, one could derive limits in the plane of $M_g - M_{LSP}$ for a specific stopped gluino model.

The jet energy ranges chosen are calculated from the resolution of the simulated samples. The signal window for each of the four samples is from M-0.5*RMS to M+2.0*RMS, where M is the mean jet energy of the sample (after all selections) and RMS is the sample's jet energy RMS. Approximately 80% of the simulated signal events fell within this window cut, depending weakly on the signal mass. An asymmetric window was chosen since the background is falling exponentially with increasing jet energy, whereas the signal is roughly symmetric in jet energy around the mean. Table I shows, for each jet energy range considered, the number of events observed in data, expected from background, the signal efficiency, and the corresponding observed and expected cross-section limits on signal jets, for a small gluino lifetime: <3 hours. The integrated luminosity was 410±20 pb^{-1}.

From the relation between the gluino and LSP masses and the observed jet energy, Equation 1, one can solve for the gluino mass and results can be translated from the generated set of signal samples to any other set of (M_g,M_{LSP}) which would give the same jet energy. We can now place upper limits on the stopped gluino cross-section vs. the gluino mass, for an assumed LSP mass, assuming a 100% BR of G→g+LSP. These can be compared with the predicted cross-sections for stopped gluinos (which includes its production and its probability to stop) taken from [3]. Three curves are drawn to represent the large theory uncertainty, resulting from the variation of the neutral to charged R-hadron conversion cross-section used. Figure 5 shows these upper limits for assumed LSP masses of 50, 90, and 200 GeV, for a small gluino lifetime: <3 hours.

If the gluino lifetime is significantly longer (on the scale of the typical store luminosity profile), the efficiency of the trigger degrades. The resulting effect on the stopped gluino cross-section limits for an LSP mass of 50 GeV is shown in Figure 6.

Thanks to Jay Wacker and L. Schwartz for very helpful inputs and discussions. We thank the staffs at Fermilab and collaborating institutions, and acknowledge support from the DOE and NSF (USA); CEA and CNRS/IN2P3 (France); FASI, Rosatom and RFBR (Russia); CAPES, CNPq, FAPERJ, FAPESP and FUNDUNESP (Brazil); DAE and DST (India); Colciencias (Colombia); CONACyT (Mexico); KRF and KOSEF (Korea); CONICET and UBACyT (Argentina); FOM (The Netherlands); PPARC (United Kingdom); MSMT (Czech Republic); CRC Program, CFI, NSERC and WestGrid Project (Canada); BMBF and DFG (Germany); SFI (Ireland); The Swedish Research Council (Sweden); Research Corporation; Alexander von Humboldt Foundation; and the Marie Curie Program.

[*] Visitor from Augustana College, Sioux Falls, SD, USA
[§] Visitor from ICN-UNAM, Mexico City, Mexico.

[‡] Visitor from Helsinki Institute of Physics, Helsinki, Finland.
[#] Visitor from Universität Zürich, Zürich, Switzerland.

[1] N. Arkani-Hamed, S. Dimopoulos, G. F. Giudice and A. Romanino, Nucl. Phys. B **709**, 3 (2005) [arXiv:hep-ph/0409232].
[2] A. C. Kraan, Eur. Phys. J. C **37**, 91 (2004) [arXiv:hep-ex/0404001].
[3] A. Arvanitaki, S. Dimopoulos, A. Pierce, S. Rajendran and J. Wacker, arXiv:hep-ph/0506242.
[4] T. Sjöstrand *et al.*, Comp. Phys. Comm. **135**, 238 (2001).
[5] G. C. Blazey *et al.*, in *Proceedings of the Workshop: "QCD and Weak Boson Physics in Run II,"* edited by U. Baur, R. K. Ellis, and D. Zeppenfeld, (Fermilab, Batavia, IL, 2000) p. 47; see Sec. 3.5 for details.